Nanostructures

Preparation of Ag_2S Nanocrystals of Predictable Shape and Size**

*Wen Pei Lim, Zhihua Zhang, Hong Yee Low, and Wee Shong Chin**

While many studies have focused on the control of the size of nanoparticles for their quantum-confined properties, the ability to synthesize monodispersed nanocrystals with predictable shape remains a challenge. The control of crystal shapes, in addition to their sizes and the higher surface-to-volume ratio, provides one more key factor to manipulate the properties of nanocrystals.[1] For example, it has been reported that the sublimation energy of Au {110} faces is significantly lower than that of Au {100} and Au {111} faces.[1b] For future applications of nanomaterials, it is foreseen that the particle shapes (i.e. the crystallographic surfaces enclosing the particles) will become an important issue.

Ag_2S is a direct, narrow band-gap semiconductor[2] with good chemical stability and excellent optical limiting properties; the optical limiting responses toward nanosecond laser pulses at 532 nm are much stronger than those of [60]fullerene and chloroaluminum phthalocyanine.[3] Ag_2S has been used in optical and electronic devices such as photovoltaic cells, photoconductors, and IR detectors,[4] and as superionic conductors.[5] To date, however, there are few reports on the preparation of Ag_2S nanocrystals with unique shapes. Herein we report on the control of the size and shape of Ag_2S nanocrystals synthesized from an easily prepared precursor under mild conditions in solution.

Controlling the shape of nanoparticles has thus far been achieved in two ways: using a template[6–9] or in solutions by employing appropriate capping agents.[10–12] The latter method is more attractive owing to higher yield and simplicity (there is no template to remove after the preparation). Among the solution methods, the injection of an organometallic precursor into a hot coordinating solvent provides a simple route to produce particles with desirable properties (e.g high crystallinity, and uniform shapes and sizes with a high degree of monodispersity).[13] However, the latter method usually involves elaborate preparation of air-sensitive organometallic complexes that decompose exothermically in

[*] W. P. Lim, Z. Zhang, Dr. W. S. Chin
Department of Chemistry
National University of Singapore
3 Science Drive 3, Singapore 117543 (Singapore)
Fax: (+65) 6779-1691
E-mail: chmcws@nus.edu.sg.
Dr. H. Y. Low
Institute of Materials Research and Engineering
3 Research Link, Singapore 117602 (Singapore)

[**] This research work was supported by the National University of Singapore Academic Research Fund R-143-000-167-112. We thank Mr. Wong Chiong Teck for his assistance in the DFT calculations.

Supporting information for this article is available on the WWW under http://www.angewandte.org or from the author.

 DOI: 10.1002/ange.200460566

air, and also the use of high temperatures. It is therefore of interest to find an easily accessible precursor that would decompose under mild conditions.

We have discovered that the air-stable precursor silver(I) thiobenzoate (Ag(SCOPh))[14] meets such requirements. The precursor crystals were found to decompose in amine at room temperature to give Ag_2S nanoparticles.[15] When a solution of the precursor dissolved in trioctylphosphine (TOP) is added under nitrogen to a warm solution (80, 100, or 120 °C) of a long-chain amine such as hexadecylamine (HDA), well-defined nanocrystals are formed, the size and shape of which can be controlled by the reaction conditions. Several parameters are identified as important and have been investigated, namely, the reaction temperature, type of amine, relative concentration of the reagents, and reaction time. The influence of these parameters on the final size and morphology of the prepared Ag_2S nanocrystals is summarized in Table 1. All the prepared nanocrystals were characterized by X-ray diffraction (XRD) and transmission electron microscopy (TEM).

Various shapes of Ag_2S nanocrystals can be readily produced, sometimes as the exclusive form, by varying the reaction temperature and amine concentration. At low temperature (80 °C), faceted Ag_2S nanocrystals are obtained when the precursor is injected into HDA. TEM images of the nanocrystals reveal a self-assembled hexagonal closed-packed array (Figure 1a). Clear lattice planes visible in the HRTEM image (Figure 1b) confirm the good crystallinity (d spacing = 2.8 Å) of the particles produced at such low temperature. The average diameter of the nanocrystals is 14.5 nm (with a size distribution of 6.2%), and the average core-to-core interparticle distance is about 19 nm (Figure 1c). In regions where two layers of these crystals overlap (Figure 1d), the hexagonal closed-packed arrays are clearly maintained in the overlayers. Such closed-packed stackings can lead to the formation of a three-dimensional self-organized superlattice assembly.[16] The selected area electron diffraction (SAED) pattern of the sample (Figure 1e) exhibits polycrystalline diffraction rings that can be indexed to the monoclinic structure of Ag_2S (see below).

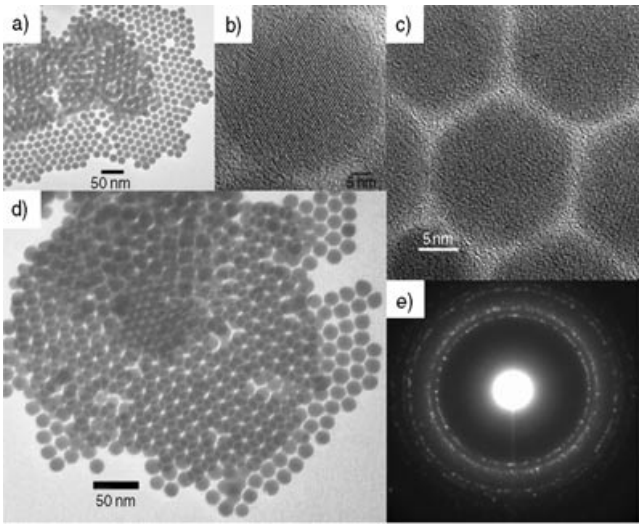

Figure 1. a) Representative TEM image of Ag_2S nanocrystals produced at 80 °C; b) and c) HRTEM images of the faceted nanocrystals; d) TEM image showing the monolayer and multilayers of the hexagonal closed-packed array of the nanocrystals; e) SAED pattern of the nanocrystals.

We have found that by increasing the injection temperature to 120 °C, cube-shaped Ag_2S crystals are obtained exclusively. The uniform Ag_2S nanocubes self-assemble into ordered two-dimensional arrays on the surface of the transmission electron microscope grid (Figure 2a). The average diameter of these nanocubes is 44.0 nm (with a size distribution of 9.8%). The scanning electron microscope (SEM) image in Figure 2b (sample coated with gold to improve contrast) illustrates that an abundant quantity of these nanocubes can be obtained by using this approach. HRTEM images (Figure 2c and d) clearly show that these Ag_2S nanocubes are single crystals with sharp lattice fringes extending to the edges.

While exclusive formation of faceted crystals and nanocubes is obtained at about 80 °C and 120 °C, respectively, mixtures of nanocubes and faceted crystals (low amine concentration) or faceted particles and nanorods (medium amine concentration) can be obtained at an injection temperature of 100 °C (Figure 3). Prolonged heating of the reaction mixtures for up to 2 h did not change the particle morphology and the particle sizes are only slightly affected.

The XRD patterns of all samples were indexed to the monoclinic acanthite Ag_2S. Nevertheless, the intensities of some diffraction lines were relatively enhanced in

Table 1: Summary of the size and shape of nanocrystals obtained under various reaction conditions.

Amine[a]	[Amine]/[precursor]	Reaction temperature [°C]	Reaction time [min]	Average size from TEM [nm]	Morphology
HDA	8:1	120	10	47.7 ± 4.2	cubes
HDA	12:1	120	10	44.0 ± 4.3	cubes
HDA	16:1	120	10	40.8 ± 5.1	cubes
HDA	20:1	120	10	31.5 ± 3.0	cubes
HDA	8:1	100	10	31.7 ± 2.6	faceted crystals & cubes
HDA	12:1	100	10	20.5 ± 2.4 (37.4 ± 4.3) × (18.6 ± 2.3)	faceted crystals & rods
HDA	16:1	100	10	25.7 ± 3.5 (46.5 ± 5.3) × (21.4 ± 3.4)	faceted crystals & rods
HDA	20:1	100	10	29.6 ± 1.5	faceted crystals
HDA	8:1	80	15	6.7 ± 0.6	faceted crystals
HDA	16:1	80	15	14.5 ± 0.9	faceted crystals
HDA	20:1	80	15	20.9 ± 1.6	faceted crystals
OA	8:1	120	10	43.0 ± 6.4	cubes
OA	20:1	120	10	39.1 ± 5.9	cubes
DOA	12:1	120	10	11.1 ± 1.9	faceted crystals
DOA	16:1	120	10	~13	not homogenous
DOA	20:1	120	10	~17	not homogenous
EDA	16:1	120	10	–	network-like

[a] HDA = hexadecylamine; OA = octylamine; DOA = dioctylamine; EDA = ethylenediamine.

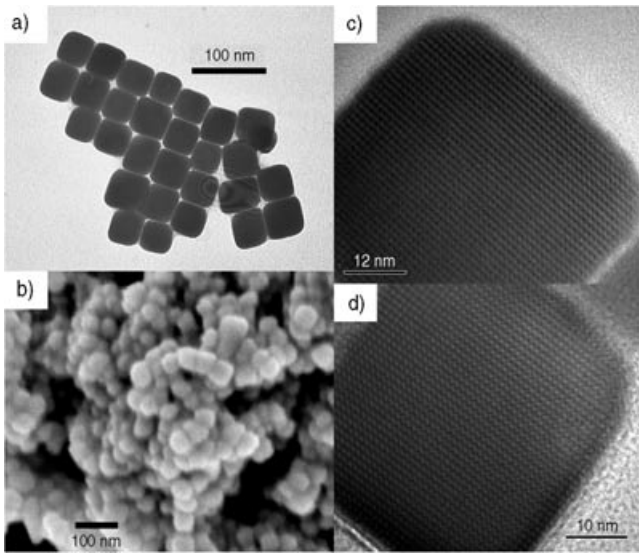

Figure 2. a) Representative TEM image of Ag_2S nanocubes produced at 120 °C; b) SEM image showing clusters of the abundant Ag_2S nanocubes; c) and d) HRTEM images showing clear lattice fringes of the nanocubes.

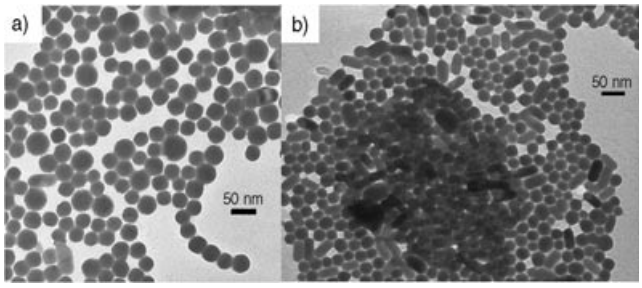

Figure 3. Representative TEM images showing a mixture of a) nanocubes and faceted nanocrystals ([HDA]/[precursor] = 8:1) and b) nanorods and faceted nanocrystals ([HDA]/[precursor] = 16:1) both obtained at 100 °C.

the faceted nanocrystals (Figure 4). Ag_2S is known to exist in three modifications: 1) the monoclinic α-phase at room temperature, 2) the body-centered cubic β-phase at temperatures between 178 and 600 °C, and 3) the face-centered cubic γ-phase above 600 °C. All these phases share a common cubic or near-cubic framework of anions, with the cations distributed at different interstitial locations.[17] It has been reported that Ag ions diffuse readily among the interstitial sites and thus lead to a facile morphological transformation.[18] We find that the enhanced diffraction peaks in Figure 4c correspond to the major lines of the cubic β-Ag_2S pattern. Hence it seems that β-phase crystals are formed under reaction conditions we employed, although the exact mechanism is unclear at the moment. This metastable phase can be detected for all faceted crystals (and mixtures) prepared at 80 and 100 °C. The formation of the β-Ag_2S phase will be of technological interest as it is known to display superionic behavior.[5]

We have found that injecting the precursor into hot TOPO (> 120 °C) alone yielded Ag nanoparticles instead of Ag_2S

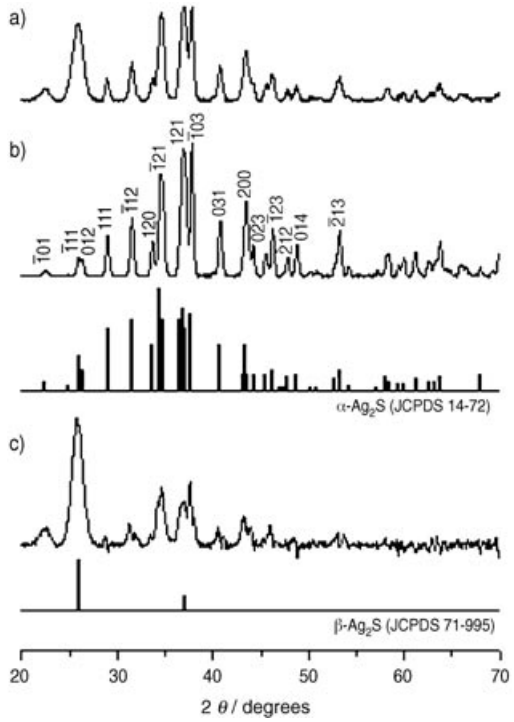

Figure 4. Representative X-ray diffraction patterns of Ag_2S: a) faceted nanocrystals formed at 80 °C, b) nanocubes formed at 120 °C, and c) the resulting pattern obtained by normalized subtraction of pattern b from pattern a. The simulated diffraction patterns from the JCPDS database are plotted for comparison.

(see Supporting Information). Hence, the amine is used here not just as the size- and shape-controlling agent, it also facilitates the decomposition of the precursor to Ag_2S [Eq. (1)]. In the presence of amine, the stronger S–C bond is broken instead of the weaker Ag–S bond;[19] we believe this is due to an initial nucleophilic attack of the amine onto the thiocarboxylate carbon atom. The reaction is best described as a degradation reaction (i.e. not a nucleophilic substitution) since the formal charges on silver (1+) and sulfur (2−) do not change while the structure of the precursor is destroyed. During the reaction, H_2S gas is evolved and an amide is isolated.[20] Theoretical calculations are now underway to provide further insight into the energetics of possible reaction pathways.

$$2\,Ag(SCOPh) + 2\,CH_3(CH_2)_{15}NH_2 \rightarrow Ag_2S + 2\,CH_3(CH_2)_{15}NHCOPh + H_2S \quad (1)$$

It is evident from Table 1 that varying the amine-to-precursor ratio provides systematic control of the size of the nanocrystals. A plot of the average particle size against amine-to-precursor ratio reveals different trends for the three injection temperatures (Figure 5). The size of the nanocrystals generated appears to be dependent on a delicate balance between the surface-capping role and the nucleophilic attacking role of HDA. Thus, while the degradation reaction readily occurs at higher temperature (120 °C), the size-controlling role of HDA dominates. As such, smaller crystals are obtained when more capping agent is present—a trend

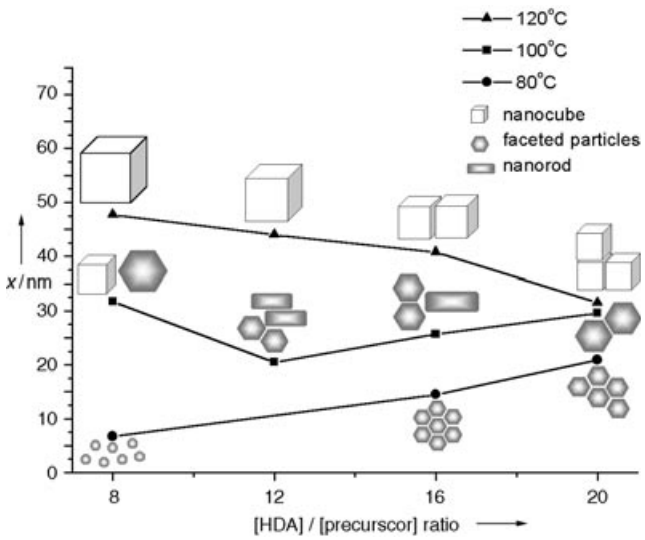

Figure 5. Effect of temperature and amine-to-precursor ratio on the shape and size of the Ag_2S nanocrystals obtained. The size of the nanorods is not included in the graph. x = particle size.

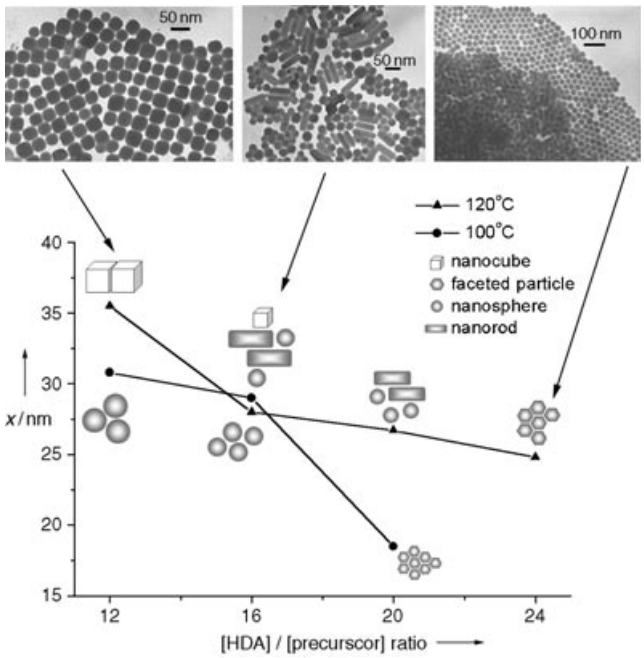

Figure 6. The shape and size of Ag_2S nanocrystals obtained by the slow heating and aging method. Effect of temperature and amine-to-precursor ratio is illustrated and typical TEM images recorded at 120 °C are shown. The size of the nanorods is not included in the graph.

that is common for most reported preparations of nanoparticles. When the temperature is low (80 °C), however, the nucleophilic attacking role of HDA becomes important. In this case, increasing the amount of HDA will increase the rate of degradation and hence an increase in the particle size occurs. At 100 °C, the two roles are competitive and we observe a steady increase in crystal size only when the amine-to-precursor ratio exceeds a certain value.

The heating rate also plays an important role in controlling the size and shape of the nanocrystals. For example, we have also prepared the nanocrystals by injecting the precursor into HDA solution at 60 °C (necessary to maintain liquid HDA) and slowly heating the reaction mixture and aging it at 100 °C (or 120 °C) for 30 min. We found that uniform particles can also be obtained but their shape and size display different trends (Figure 6; details in Supporting Information).

Thus, one may summarize the morphology control as follows: 1) formation of nanocubes is favored at high temperature (120 °C) or low amine concentration; 2) faceted nanocrystals are favored at low temperature (80 °C) or high amine concentration; 3) elongated structures are obtained with medium amine concentration at 100–120 °C. Recent studies have shown that morphology control of nanocrystals can be effected through a delicate balance of the nucleation and growth rate.[21] In particular, preferential growth of particular crystallographic surfaces is possible during kinetically controlled growth processes.[21a] In the method here, we note that the nucleation rate is also dependent on the amine concentration since the degradation of the precursor is not a simple thermolysis process. It seems that the formation of cube-shaped Ag_2S crystals is thermodynamically driven and favored by low monomer concentration (i.e. low amine concentration). At 120 °C, the sticking coefficient of capping HDA molecules is less selective and hence isotropic crystals are produced. The formation of faceted and elongated Ag_2S nanocrystals seems to be a kinetically driven reaction and is favored at high monomer concentration. This nonequilibrium kinetic-growth regime is further supported by the formation of the metastable β-phase along with these anisotropic crystals. As evident in Table 1, the nature and type of amine are found to be important also in the shape control. Thus, formation of nanocubes is only observed at 120 °C in HDA and octylamine (OA) but not in dioctylamine (DOA) or ethylenediamine (EDA). Since the nucleophilicity of these amines is similar, we believe that steric effects are playing a role here. This aspect is currently under investigation.

In conclusion, we have described an unprecedented amine-mediated reaction for preparing Ag_2S nanocrystals under mild conditions. By controlling a few critical parameters, a simple route that provides Ag_2S nanocrystals of predictable size and shape is presented. Our preliminary investigations show that this general route can also be applied to the preparation of other chalcogenide nanocrystals.

Experimental Section

Unless otherwise stated, all materials were purchased from commercial sources and used without further purification. All procedures were carried out by using standard techniques under a nitrogen atmosphere. Hexadecylamine (HDA) was dried and degassed at 120 °C before use. A degassed solution of Ag(SCOPh) (0.025 g) in TOP (0.2 mL) was injected into a hot solution (80 °C/100 °C/120 °C) of HDA. After these components had been mixed, the pale yellow solution rapidly changed to brown. After 10 min, the reaction solution was cooled to room temperature, then toluene (ca. 1 mL) was added and the product was precipitated by addition of methanol. The precipitate was centrifuged, washed thoroughly with methanol, and dried in vacuum overnight. Alternatively, Ag(SCOPh) was introduced into HDA at 60 °C and the mixture was heated to the desired

temperature (100 °C/120 °C) and aged at that temperature for 30 min. The XRD pattern was acquired by using a Bruker D5005 diffractometer with $Cu_{K\alpha}$ radiation ($\lambda = 0.151478$ nm). TEM was performed on a Philips CM100 microscope operating at 100 kV, and HRTEM was performed on a Philips CM300 FEG instrument with an acceleration voltage of 300 kV. SEM images were obtained by using a JEOL JSM6700 microscope, operating at 10 amp and 15 kV.

Received: May 6, 2004
Revised: July 23, 2004

Keywords: chalcogenides · crystal growth · electron microscopy · nanostructures

[1] a) Z. L. Wang, *J. Phys. Chem. B* **2000**, *104*, 1153; b) M. B. Mohamed, Z. L. Wang, M. A. El-Sayed, *J. Phys. Chem. A* **1999**, *103*, 10255.
[2] K. Akamatsu, S. Takei, M. Mizuhata, A. Kajinami, S. Deki, S. Takeoka, M. Fujii, S. Hayashi, K. Yamamoto, *Thin Solid Films* **2000**, *359*, 55.
[3] Y. P. Sun, J. E. Riggs, H. W. Rollins, R. Guduru, *J. Phys. Chem. B* **1999**, *103*, 77.
[4] a) G. Hodes, J. Manassen, D. Cahen, *Nature* **1976**, *261*, 403; b) S. Kitova, J. Eneva, A. Panov, H. Haefke, *J. Imaging Sci. Technol.* **1994**, *38*, 484.
[5] a) S. Hull, D. A. Keen, D. S. Sivia, P. A. Madden, M. Wilson, *J. Phys. Condens. Matter* **2002**, *14*, 9; b) T. Minami, *J. Non-Cryst. Solids* **1987**, *95*, 107.
[6] J. Bao, D. Xu, Q. Zhou, Z. Xu, *Chem. Mater.* **2002**, *14*, 4709.
[7] J. C. Hulteen, C. R. Martin, *J. Mater. Chem.* **1997**, *7*, 1075.
[8] a) W. Han, P. Kohler-Redlich, C. Scheu, F. Ernst, M. Rühle, N. Grobert, M. Terrones, H. W. Kroto, D. R. M. Walton, *Adv. Mater.* **2000**, *12*, 1356; b) J. Bao, K. Wang, Z. Xu, H. Zhang, Z. Lu, *Chem. Commun.* **2003**, *2*, 208.
[9] a) J. Tanori, M. P. Pileni, *Langmuir* **1997**, *13*, 639; b) M. P. Pileni, T. Gulik-Krzywicki, J. Tanori, A. Filankembo, J. C. Dedieu, *Langmuir* **1998**, *14*, 7359.
[10] a) V. F. Puntes, K. M. Krishnan, A. P. Alivisatos, *Science* **2001**, *291*, 2115; b) N. R. Jana, L. Gearheart, C. J. Murphy, *Adv. Mater.* **2001**, *13*, 1389; c) B. Nikoobakht, M. A. El-Sayed, *Chem. Mater.* **2003**, *15*, 1957.
[11] a) T. S. Ahmadi, Z. L. Wang, T. C. Green, A. Henglein, M. A. El-Sayed, *Science* **1996**, *272*, 1924; b) J. M. Petroski, Z. L. Wang, T. C. Green, M. A. El-Sayed, *J. Phys. Chem. B* **1998**, *102*, 3316; c) Y. Sun, Y. Xia, *Science* **2002**, *298*, 2176.
[12] K. K. Caswell, C. M. Bender, C. J. Murphy, *Nano Lett.* **2003**, *3*, 667.
[13] a) C. B. Murray, D. J. Norris, M. G. Bawendi, *J. Am. Chem. Soc.* **1993**, *115*, 8706; b) B. O. Dabbousi, J. Rodriguez-Viejo, F. V. Mikulec, J. R. Heine, H. Mattoussi, R. Ober, K. F. Jensen, M. G. Bawendi, *J. Phys. Chem. B* **1997**, *101*, 9463; c) D. V. Talapin, S. Haubold, A. L. Rogach, A. Kornowski, M. Hasse, H. Weller, *J. Phys. Chem. B* **2001**, *105*, 2260; d) J. Hambrock, A. Birkner, R. A. Fischer, *J. Mater. Chem.* **2001**, *11*, 3197.
[14] V. V. Savant, J. Gopalakrishnan, C. C. Patel, *Inorg. Chem.* **1969**, *8*, 748.
[15] Z. H. Zhang, W. P. Lim, C. T. Wong, F. F. Yin, W. S. Chin, unpublished results.
[16] a) M. P. Pileni, *Appl. Surf. Sci.* **2001**, *171*, 1; b) M. P. Pileni, *J. Phys. Chem. B* **2001**, *105*, 3358; c) L. Motte, F. Billoudet, E. Lacaze, J. Douin, M. P. Pileni, *J. Phys. Chem. B* **1997**, *101*, 138.
[17] R. J. Cava, D. B. McWhan, *Phys. Rev. Lett.* **1980**, *45*, 2046, and references therein.
[18] R. L. Allen, E. J. Moore, *J. Phys. Chem.* **1959**, *63*, 223, and references therein.
[19] Preliminary results from DFT B3LYP//LANL2DZ calculations showed that the bond dissociation energy of AgS–COPh is 265.95 kJ mol^{-1}, whereas that of Ag–SCOPh is 206.41 kJ mol^{-1}.
[20] Isolation of $CH_3(CH_2)_{15}NHCOPh$: The product was purified by preparative TLC and recrystallized from chloroform/hexane. ^{1}H NMR ($CDCl_3$): $\delta = 0.88$ (t, $J = 6.6$ Hz, 3H; CH_3), 1.26 (s, 26H; CH_2), 1.59 (quin, 2H; $NHCH_2CH_2$), 3.46 (q, $J = 6.7$ Hz, 2H; $NHCH_2$), 6.08 (br, 1H; NH), 7.40–7.52 (overlapping t, 3H; *m*-,*p*-Ph), 7.75 ppm (d, $J = 6.8$ Hz, 2H; *o*-Ph); ^{13}C NMR ($CDCl_3$): $\delta = 14.0$ (CH_3), 22.6 (CH_2CH_3), 26.9 ($NCH_2CH_2CH_2$), 29.2–29.6 (CH_2), 31.8 (NCH_2CH_2), 40.0 (NCH_2), 126.7 (*o*-Ph), 128.4 (*m*-Ph), 131.2 (*p*-Ph), 167.8 ppm (-C=O); elemental analysis (%) calcd: C 79.94, H 11.38, N 4.05; found: C 80.13, H 10.92, N 4.24.
[21] a) S-M Lee, S-N Cho, J. Cheon, *Adv. Mater.* **2003**, *15*, 441; b) Z. A. Peng, X. Peng, *J. Am. Chem. Soc.* **2002**, *124*, 3343; c) W. W. Yu, Y. A. Wang, X. Peng, *Chem. Mater.* **2003**, *15*, 4300.

